Turkish Journal of Electrical Engineering & Computer Sciences

http://journals.tubitak.gov.tr/elektrik/

Research Article

Turk J Elec Eng & Comp Sci
(2017) 25: 3273 – 3288
© TÜBİTAK
doi:10.3906/elk-1603-17

A particle swarm optimization and block-SVD-based watermarking for digital images

Falgun THAKKAR*, **Vinay Kumar SRIVASTAVA**
Department of Electronics and Communication Engineering, Motilal Nehru National Institute of Technology, Allahabad, India

Received: 02.03.2016 • **Accepted/Published Online:** 30.12.2016 • **Final Version:** 30.07.2017

Abstract: The major issues in most watermarking schemes are security, reliability, and robustness against attacks. To achieve these objectives in a watermarking algorithm, the selection of a scale factor to embed the watermark into the host image is a challenging problem. In this paper, a block singular value decomposition (SVD)-based reliable, robust, secure, and fast watermarking scheme is proposed that uses particle swarm optimization (PSO) in the selection of the scale factor. SVD is applied here on the nonoverlapping blocks of LL wavelet subbands. Selected singular values of these blocks are modified with the pixel values of the watermark image. Selected locations of these singular values increase security. In addition, the scale factor using PSO for embedding the watermark increases the robustness and imperceptibility of the proposed scheme. Direct embedding of the watermark image into the host image and the use of block-SVD makes the scheme faster. Comparative analysis with an existing algorithm shows that the proposed technique performs well during most types of noise attacks and removes the diagonal line problem present in the extracted watermark image.

Key words: Adaptive image watermarking, particle swarm optimization, block singular value decomposition, security, discrete wavelet transform, normalized similarity ratio

1. Introduction

The reproduction of digital data is possible without any loss, but they are not robust against intentional attacks and malicious tampering. Therefore, digital multimedia communication requires a type of scheme that can provide authentication and rightful ownership protection to these data [1,2].

Rightful ownership and resistance against common attacks are achieved using singular value decomposition (SVD)-based image watermarking [1]. However, it was proved in [3,4] that this SVD-based method cannot completely protect rightful ownership. The drawback of SVD-based watermarking techniques reported in [3,4] was removed in [5] using principal components (PCs). In this technique [5], in place of singular values, the PCs are embedded into the cover image. To improve rightful ownership protection and robustness, the watermark image is directly embedded into the singular values of (HL) and (LH) wavelet subbands of the cover image [6]. The discrete wavelet transform (DWT), SVD, and SVD-DWT-based watermarking techniques are applied to medical images and compared in [7]. Direct embedding of the watermark into the block-wise SVD of the cover image makes the algorithm not only free from false-positive problems but also enhances its robustness [8–11]. The block-based SVD is applied in the spatial domain as well as in the transform domain [12] to increase the security and robustness of the algorithm. A novel block DWT-based watermarking scheme was proposed in [13],

*Correspondence: falgungcet@gmail.com

in which the vector image is used as a watermark and embedded into the blocks of DWT subbands of the cover image with a size of 8 $\times$ 8. It can be observed that the extracted watermark image is quite close to the original watermark against a variety of attacks. A comparative study of block-based discrete cosine transform (DCT) and DWT watermarking approaches was given with significant remarks on the effect of JPEG and JPEG 2000 compression in [14].

A watermarking technique using particle swarm optimization (PSO) was introduced for embedding and extraction of watermark content in [15]. Appropriate selection of a scale factor for watermark embedding into the host image is a challenging task to devise better watermarking schemes in terms of imperceptibility, robustness, security, and reliability. A comparative analysis of a watermarking scheme based on a genetic algorithm (GA), PSO, and hybrid PSO (HPSO) was given in [16] to attain a suitable scale factor. This analysis shows that the HPSO-based technique is more reliable compared to other techniques, but it is more complex. The GA has been used to embed the image watermark in audio signals [17]. It is used to determine the quantization step for embedding permuted images into selected coefficients of the audio signal. An embedding equation as well as a scale factor for embedding the watermark in DCT coefficients of the cover image were generated by a GA in [18]. This scheme provides a balance between robustness and imperceptibility. To remove false-positive problems from SVD-based watermarking techniques, PCs are embedded into the transform coefficients of a cover image using a 2D scale factor [19,20]. This scale factor is optimized with the help of a metaheuristic algorithm PSO. The trade-off between invisibility and robustness is obtained using PSO while embedding the watermark into wavelet packet coefficients of the cover image [21]. Block-SVD is applied on the LL subband of the cover image, and watermark bits are embedded into certain elements of U matrices [22]. Watermark contents are estimated for the U matrix using a support vector machine (SVM) and PSO. The scheme is robust but complex due to the training part needed for watermark extraction. PSO is used in the selection process of wavelet coefficients of the host image for watermark embedding in [23]. PSO is subjected to different attacks in this study to obtain robustness and imperceptibility.

The watermarking scheme proposed in this paper is based on block-SVD, DWT, and the PSO algorithm. The use of block-SVD not only increases the robustness and security of the proposed algorithm but also removes the diagonal line problem found in the extracted watermark. PSO makes the proposed algorithm adaptive to a variety of cover images and noise attacks. A DWT-SVD-based watermarking scheme using PSO was proposed in [24] to get better robustness. In this scheme, instead of a direct watermark, the SVs of the watermark image are embedded into the SVs of wavelet subbands of the cover image, which leads to a false-positive problem in the extracted watermark [24]. Moreover, for watermark embedding, the SVs of all wavelet subbands of the cover image are modified, which increases robustness along with complexity. Therefore, compared to the scheme in [24], the scheme proposed in this paper is better in terms of computational complexity and rightful ownership due to direct embedding of the watermark image into blocks of LL subband only.

In [24], SVD was applied on all the wavelet subbands, namely LL, LH, HL and (HH), of the cover image and watermark image. The singular values of each wavelet subband are modified by the singular values of the watermark image in order to embed it, allowing the scheme to have a good embedding capacity. A suitable scale factor for the same image is selected using PSO iteratively until the desired value of the watermarking parameters is achieved. In this process, the computational complexity of the algorithm increases because the four copies of the watermark singular values are required to be embedded into the cover image even though this increases robustness. The total number of PSO iterations is also not specified, which may lead to more computations.

PSO-based watermarking was also proposed in [22] using DWT, SVD, and support vector regression (SVR). In the proposed algorithm, watermark bits are directly embedded into the U matrix of the LL subband of the cover image. The watermark is extracted using SVR, whose optimal parameters for training are selected using the PSO algorithm. During the process of watermark extraction, this training pattern is utilized. This algorithm is able to deal with the false-positive problem of SVD-based watermarking, but it is complex due to the use of SVR. This scheme is robust and blind due to the use of the SVR technique.

In the scheme proposed in this paper, watermark bits are directly embedded into the highest singular value of the nonoverlapping blocks of an LL subband. This modification of singular values is done with watermark bits weighted by the appropriate scale factor. This scale factor is chosen using the PSO algorithm. Inverse SVD is then applied to reconstruct the modified LL subband. The watermarked image is formed using inverse wavelet transform on the modified LL subband and remaining subbands of the cover image. During watermark extraction, the same process is performed in reverse order. Although several benefits are achieved with the proposed algorithm, including the removal of false-positives, it has limited payload capacity. The scheme is less complex as PSO needs lower numbers of particles and iterations for any image.

The rest of the paper is organized as follows: in Section 2, preliminaries such as PSO, SVD, and DWT are discussed. The motivations behind the proposed scheme as well as the watermark embedding and extraction algorithms are described in Section 3. Performance measures are given in Section 4. Results and related analysis are given in Section 5, and conclusions are given in Section 6.

2. Preliminaries

The fundamentals of DWT, SVD, and PSO are discussed in this section as they are used in the proposed algorithm.

2.1. Discrete wavelet transform

DWT provides a multiresolution analysis of an image. The 2D-DWT on the image generates different frequency subbands with constant bandwidth on the logarithmic scale [6]. The single level of wavelet decomposition on the image generates LL, HL, LH, and HH subbands. The LL subband contains low-resolution approximate coefficients whereas the HL, LH, and HH subbands contain higher resolution coefficients in horizontal, vertical, and diagonal directions, respectively. To attain another level of subbands, the low-pass LL subband is further decomposed. This process continues until the required levels of decomposition are reached.

2.2. Singular value decomposition

In SVD, a real matrix A is decomposed into three matrices U, S, and V. The matrix S is a diagonal matrix whereas the matrices U and V are left- and right-singular matrices. The U and V matrices are orthogonal and contain geometrical information about the image whereas the singular matrix S contains intensity-related information about the image [25]. The mathematical formulation for decomposition of matrix A is given by the following equation:

$$A = s_1 U_1 V_1^T + s_2 U_2 V_2^T + \ldots + s_r U_r V_r^T. \tag{1}$$

The rank of matrix A is denoted by r in Eq. (1). U_1, $U_2 \ldots U_r$ and $V_1, V_2 \ldots V_r$ are columns of left- and right-singular values of U and V whereas s_1, $s_2 \ldots s_r$ are scalar singular values of diagonal matrix S.

SVD is often used in watermarking techniques because the singular values modified to embed the watermark are less affected by most noise attacks [25].

2.3. Particle swarm optimization

The concept of PSO was introduced for optimization of nonlinear functions in [26]. PSO is an optimization technique based on a population known as a swarm. Each member of the swarm is identified by a particle. All particles in the population present a possible solution for the optimization problem. Each particle moves towards its own personal best solution through each iteration. One of the particles of this swarm is also moving towards a global best solution.

To understand the process of this technique, let us consider a swarm of size N where each particle j in the search space has a current particle position given by x_j, current velocity v_j, and personal best position p_j. All the particles of the swarm are revised and updated using the following equations:

$$v_j(n+1) = m\left[w_j(n) * v_j(n) + c_1 * r_1(p_j - x_j(n)) + c_2 * r_2(p_{gb} - x_j(n))\right] \tag{2}$$

$$x_j(n+1) = x_j(n) + v_j(n+1) \tag{3}$$

In the above equations, n is the current iteration number, c_1 and c_2 are the acceleration constant, r_1 and r_2 are constants with a range of ($0 < r_1,\ r_2 < 1$), and p_{gb} is the global best solution. To control the particle in the search space, the velocity vector v_j is clamped to a particular range defined by $[v_{\min}, v_{\max}]$. The constants c_1 and c_2 control particle movement and have values approximately equal to 2. w is the inertia weight that is used to control the convergence during the iteration and it varies according to the following equation:

$$w_i = w_{\max} - \frac{w_{\max} - w_{\min}}{k_{\max}} \cdot k. \tag{4}$$

$k_{\max}$ and k are the maximum number of iterations and current iteration number, respectively. To assure convergence of the PSO algorithm, the value of m is decided by the following equation:

$$m = \frac{2}{\left|2 - \tau - \sqrt{\tau^2 - 4\tau}\right|} \text{where } \tau = c_1 + c_2 \text{ and } \tau \geq 4. \tag{5}$$

3. Proposed algorithm

In [27], a robust and imperceptible watermarking algorithm is presented, but the value of the scale factor is obtained from tabular analysis over a range of scale factors using only two cover images. Therefore, the analysis of the algorithm proposed in [27] is limited to a small set of images. Moreover, the algorithm does not use any technique to get a proper value of a scale factor that can provide better imperceptibility and robustness for a variety of cover images. The diagonal line problem is also present in the extracted watermark image.

The algorithm proposed in this paper provides a solution to various problems associated with the watermarking technique given in [27]. The proposed algorithm is based on block-SVD and PSO, in which the binary watermark image is directly embedded into a singular matrix obtained from the block-SVD of the LL subband of the cover image. From an analysis of optimization techniques for image watermarking, it was found that PSO performs better compared to the GA [28]. In this scheme, PSO is incorporated to get better imperceptibility and robustness. For watermark embedding, the LL subband in wavelet decomposition is robust against different noise attacks, and the small change in singular values of this subband does not significantly affect imperceptibility [27]. The LL subband is therefore selected for watermark embedding in the proposed scheme in this paper. The LL subband is divided into nonoverlapping blocks of size 4 $\times$ 4 and SVD is applied to each of them. For embedding, the watermark pixels modify the first or largest singular value of each of these blocks with a suitable scale factor. The location of embedding the watermark pixels into each block can be changed and made random to increase the security. The PSO algorithm adaptively selects a suitable value of the scale factor. The use of PSO for proper selection of the scale factor makes the proposed algorithm more generalized for a variety of cover images. Furthermore, the use of block-SVD in the embedding process not only increases imperceptibility, robustness, and security but also eliminates the diagonal line problem from the extracted watermark image.

3.1. Proposed watermark-embedding algorithm

The procedure of the proposed watermark-embedding algorithm is given below, and the block diagram of the same is shown in Figure 1.

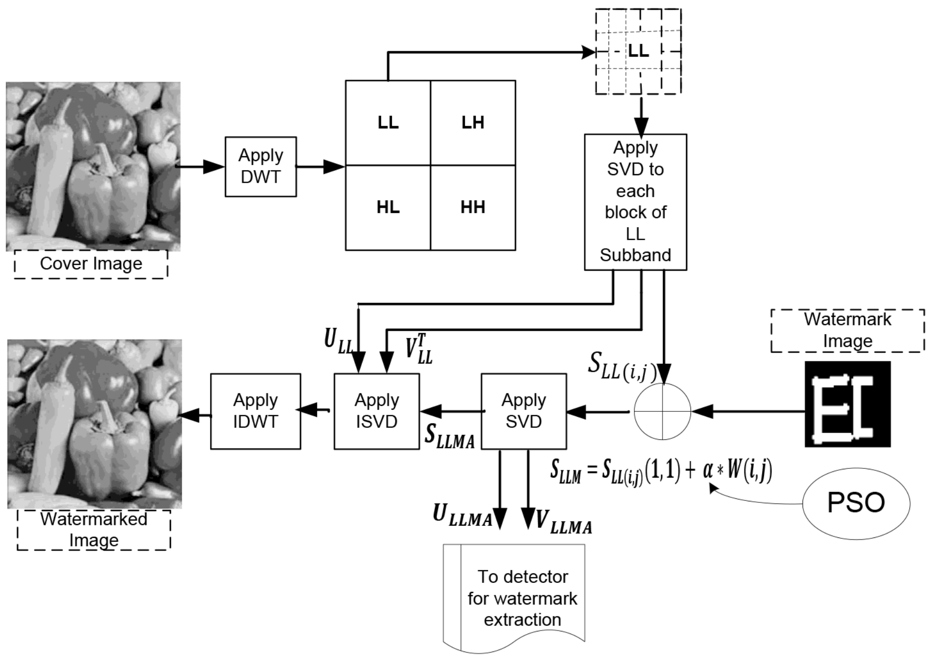

Figure 1. Block diagram of the proposed watermark embedding scheme.

Step 1. Decompose the cover image H into LL, HL, LH, and HH subbands using DWT.

Step 2. Divide the low frequency subband LL into nonoverlapping blocks of size 4×4. Let each block be represented by $LL_{(i,j)}$.

Step 3. Apply SVD to each block $LL_{(i,j)}$ as

$$[U_{LL(i,j)} S_{LL(i,j)} V_{LL(i,j)}] = LL_{(i,j)}. \tag{6}$$

Step 4. Modify the first and largest singular value of each block $S_{LL(i,j)}$ by a pixel of the watermark image using scale factor α obtained through PSO:

$$S_{LLM(i,j)} = S_{LL(i,j)}\,(1,1) + \alpha * w(ij). \tag{7}$$

Step 5. Apply block-SVD to each block $S_{LLM(i,j)}$:

$$[U_{LLMA(i,j)} S_{LLMA(i,j)} V_{LLMA(i,j)}] = S_{LLM(i,j)}. \tag{8}$$

Step 6. Apply inverse block-SVD on singular value matrices $S_{LLMA(i,j)}$ using the orthogonal matrices $U_{LL(i,j)}$ and $V_{LL(i,j)}$ to reconstruct the modified LL* subband:

$$LL^* = U_{LL(i,j)} * S_{LLMA(i,j)} * V^T_{LL(i,j)}. \quad (9)$$

Step 7. Apply inverse discrete wavelet transform on this modified LL* subband along with HL, LH, and HH subbands to get the watermarked image H^*.

3.2. Proposed watermark-extraction algorithm

The watermarked image H^* suffers from a variety of noise attacks and becomes noisy watermarked image $H^{*\prime}$. A detailed procedure to extract the watermark from $H^{*\prime}$ is given below, and the block diagram for the same procedure is shown in Figure 2.

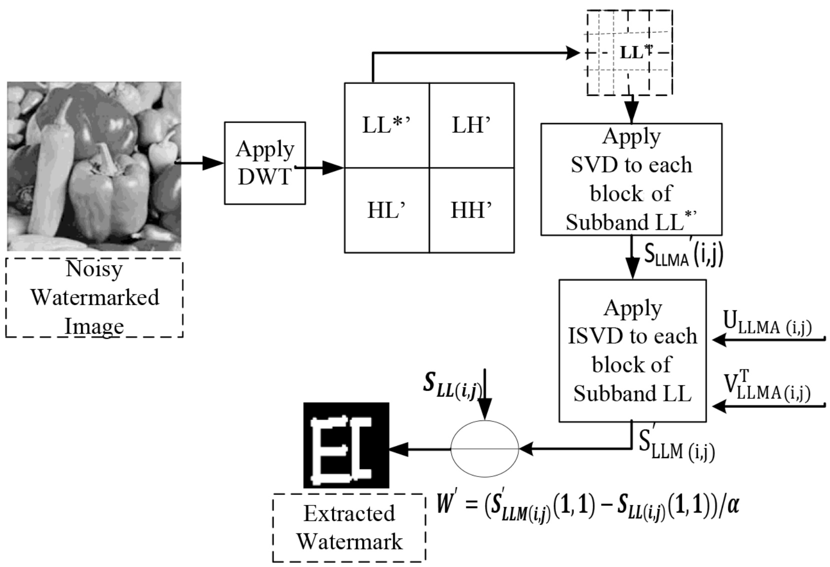

Figure 2. Block diagram of the proposed watermark extraction scheme.

Step 1. Decompose the noisy watermarked image $H^{*\prime}$ into four wavelet subbands: LL$^{*\prime}$, HL$'$, LH,$'$ and HH$'$.

Step 2. Partition the LL$^{*\prime}$ subband into nonoverlapping blocks of size 4 $\times$ 4.

Step 3. Apply SVD to each block $LL^{*\prime}_{(i,j)}$ to get modified blocks of singular values $S\prime_{LLMA(i,j)}$:

$$[U_{LL(i,j)}{}'S_{LLMA(i,j)}{}'V_{LL(i,j)}{}'] = LL^{*\prime}_{(i,j)} \quad (10)$$

Step 4. Apply inverse SVD to each block $S\prime_{LLMA(i,j)}$ along with their corresponding matrices $V_{LLMA(i,j)}$ and $U_{LLMA(i,j)}$ to get the blocks of singular matrices $S\prime_{LLM(i,j)}$:

$$S'_{LLM(i,j)} = U_{LLMA(i,j)} \times S'_{LLMA(i,j)} \times V^T_{LLMA(i,j)}. \quad (11)$$

Step 5. To extract the watermark image, find the difference between the first singular values of the set of corresponding blocks $S'_{LLM(i,j)}$ and $S_{LL(i,j)}$ using the following equation:

$$w' = (S'_{LLM(i,j)}(1,1) - S_{LL(i,j)}(1,1))/\alpha. \quad (12)$$

In the above equation, $S_{LL(i,j)}$ is a block of the singular matrix of the LL subband of the cover image obtained during the embedding process.

As the inserted watermark is a binary image, the pixels of $w\prime$ are considered equal to 1 if they are greater than 0.5 and 0 if less than 0.5.

Thus, after thresholding the extracted watermark image, $w\prime$ is obtained.

3.3. Application of PSO to find the scale factor

The robustness and imperceptibility of any watermarking algorithm mainly depend on the value of the scale factor. A small value of the scale factor increases the imperceptibility of a watermarked image, but it degrades the quality of the extracted watermark and vice versa. In most watermarking algorithms, the scale factor is kept constant and its value is selected manually for a particular group of images that may not be suitable for other group of images. As a result, to make a watermarking scheme appropriate for a variety of images, some accurate and adaptive algorithms are required to calculate the suitable value of the scale factor. In this paper, an efficient optimization algorithm, PSO, is therefore incorporated with a block-SVD-based watermarking scheme that can accurately tune the scale factor with less execution time.

To incorporate PSO in the watermarking algorithm, an initial population is generated using a random function. The population is initialized with five elements with values ranging from 0 to 150 using one of these elements as the scale factor successively one after the other, the watermark image is embedded inside the blocks of the LL subband of the cover image. Five watermarked images are generated as a result. Different noise attacks are applied to the generated watermarked images, and the watermarks are extracted using the proposed extraction algorithm. The performance of each scale factor of this population is compared using the fitness function given in Eq. (13). The maximum value of the fitness function is identified and the respective element is the global best particle, which is also known as the *gbest* particle. In this first generation, each and every particle acts as a personal best particle known as *pbest*. The next generation is created from the particles of the current generation using Eqs. (2) and (3). The performance of the elements of this generation is again tested using the fitness function. The achieved values of the respective fitness functions are compared with the values of the fitness function from the previous generation of respective elements. The elements that provide the maximum fitness values are known as *pbest* particles, and the best of these *pbest* particles is the global best particle called *gbest*. This process continues until the desired number of iterations is reached. The functional block diagram of PSO used in this paper is shown in Figure 3.

In the proposed scheme, maximum fitness is achieved at the end of the final iteration. The mathematical formula for the fitness function is given in following equation:

$$fitness = \frac{\max\left[Corr\left(w, w'\right) + Corr\left(H, H^{*}\right)\right]}{2}. \tag{13}$$

In the above equation, *Corr* indicates the normalized correlation coefficient. Variables w and H represent the watermark, and cover images w' and H^{*} are the extracted watermark and watermarked images, respectively. The various parameters of PSO are chosen and given below:

The values of both acceleration coefficients c_1 and c_2 are taken as 2.

The minimum and maximum velocities $V_{\min}$ and $V_{\max}$ are taken as 10 and 80, respectively.

The total number of particles is 5, and the number of iterations is 8.

The initial values of velocity V and inertia weight W are 50 and 0.9, respectively.

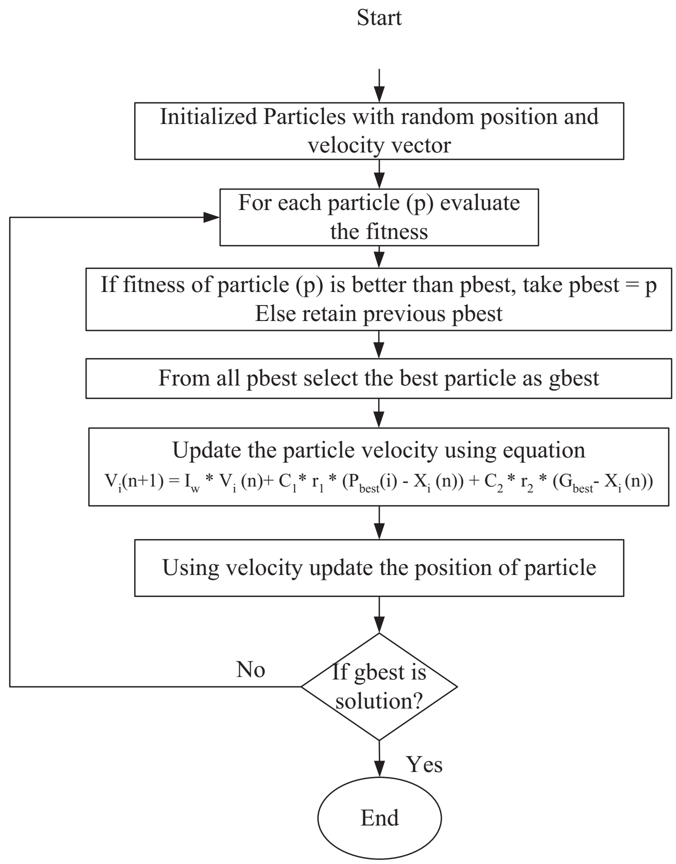

Figure 3. Flow chart of the PSO algorithm used in proposed scheme.

The value of constant m is taken as per Eq. (5) whereas inertia changes in terms of iteration, as per Eq. (4).

4. Performance measures

Performance parameters such as the normalized correlation coefficient (NCC), the peak signal-to-noise ratio (PSNR), and the normalized similarity ratio (NSR) are discussed here. The PSNR is used as a measure of imperceptibility for the watermarked image whereas the NCC and NSR are used as measures of robustness of the extracted watermark image.

The mathematical formulae of the NCC and PSNR are given below.

$$NCC = \frac{\sum_{i=1}^{N}\sum_{j=1}^{N}\left(w_{ij}-\overline{w}\right)\left(w_{ij}^{*}-\overline{w}^{*}\right)}{\sqrt{\sum_{i=1}^{N}\sum_{j=1}^{N}\left(w_{ij}-\overline{w}\right)^{2}}\sqrt{\sum_{i=1}^{N}\sum_{j=1}^{N}\left(w_{ij}^{*}-\overline{w}^{*}\right)^{2}}} \tag{14}$$

w and w^* are the original and extracted watermark images, respectively, whereas:

$$\overline{w} = \frac{1}{N^2}\sum_{i=1}^{N}\sum_{j=1}^{N} w_{ij} \text{ and } \overline{w}^* = \frac{1}{N^2}\sum_{i=1}^{N}\sum_{j=1}^{N} w_{ij}^*.$$

$$PSNR = 10\log_{10}\frac{255^2}{MSE}, \text{ where } MSE = \frac{1}{M^2}\sum_{i=1}^{M}\sum_{j=1}^{M}\left[H\left(i,j\right) - H^*\left(i,j\right)\right]^2. \tag{15}$$

Another robustness parameter, the NSR, is defined as:

$$NSR = \frac{SR - \min\left(SR\right)}{1 - \min\left(SR\right)} \text{ where } SR = \frac{S}{S+D}. \tag{16}$$

In Eq. (16), SR is the similarity ratio. In this equation, S represents the number of similar pixels whereas D represents the number of dissimilar pixels present in the original and extracted watermark images. min(SR) is the SR calculated for the original binary watermark image with the image that contains pixel values either represented as zeros (completely black) or ones (completely white) [27]. In the proposed scheme, min(SR) is calculated using the original watermark and the complete black image.

5. Results and discussion

Experimental analysis is conducted on different cover images such as Goldhill Pepper, Cameraman Lena, Baboon, and Boat at a pixel size of 512 × 512 whereas the EC logo, at 64 × 64 pixels, is used as the watermark image shown in Figure 4.

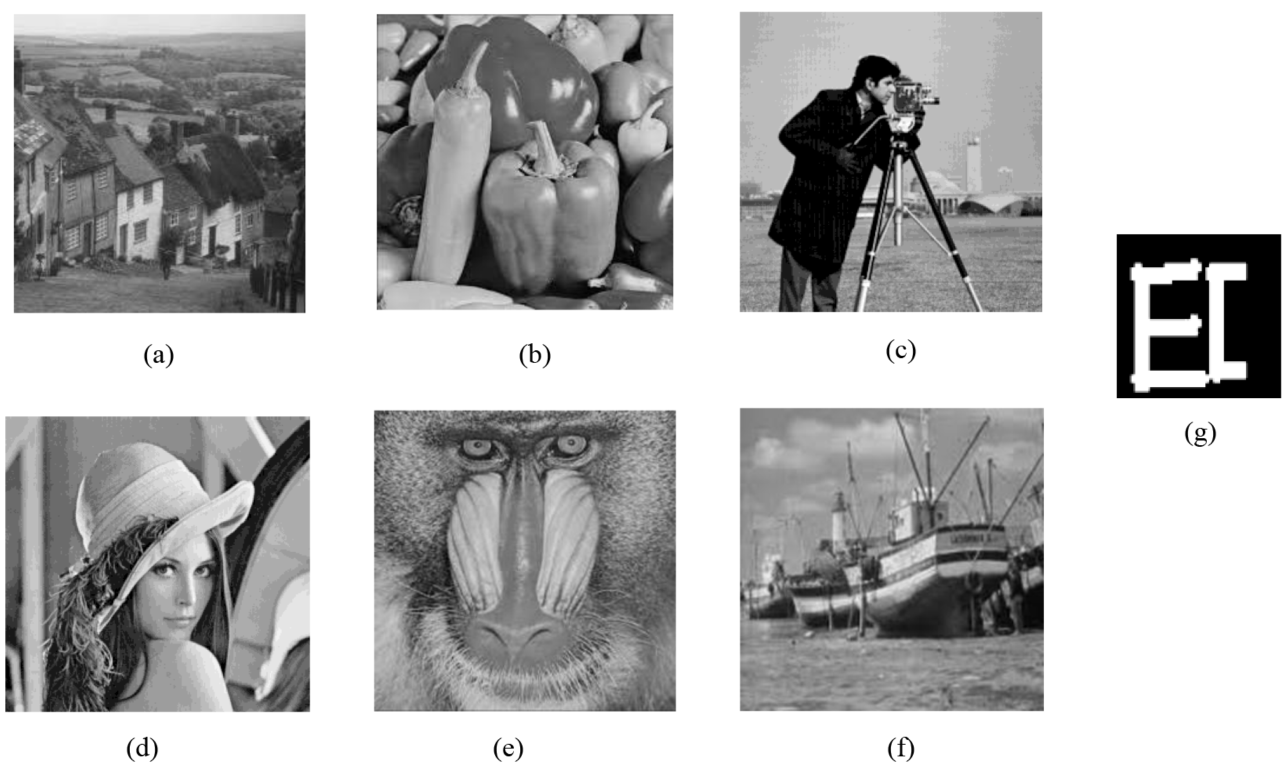

Figure 4. Cover images: a) Goldhill, b) Pepper, c) Cameraman, d) Lena, e) Baboon, f) Boat and watermark images, g) EC logo.

The analysis of PSNR value comparison between the proposed and existing algorithm [27] for the Goldhill watermarked image under different attacks is shown in Table 1, and graphical analysis for watermarked image

Pepper is given in Figure 5. The analysis shows that, for the Pepper and Goldhill watermarked images, the proposed algorithm outperforms the original under all attacks except histogram equalization and rotation attacks. During the rotation attack, the PSNR values of the proposed as well as the existing algorithm in [19] are quite close for both cover images, which is also shown in Table 1.

Table 1. PSNR comparison of the proposed and existing algorithm [27].

Attacks	PSNR (dB)	
	Watermarked image (Goldhill)	
	Reference [27]	Proposed
Gaussian blurring (3 × 3)	29.863	34.4528
Scaling (512–256)	29.7727	33.2454
Histogram eq.	17.5452	16.6719
Rotation (20°)	11.4089	10.1630
JPEG compression (Q = 25)	8.3348	26.8778
Cropping (13%)	13.0455	15.1750
Salt and pepper	12.3335	24.2177
Intensity adjustment	23.6482	22.7493
Gamma correction (0.9)	20.1435	22.7497
Median filtering (3 × 3)	32.8472	34.3906

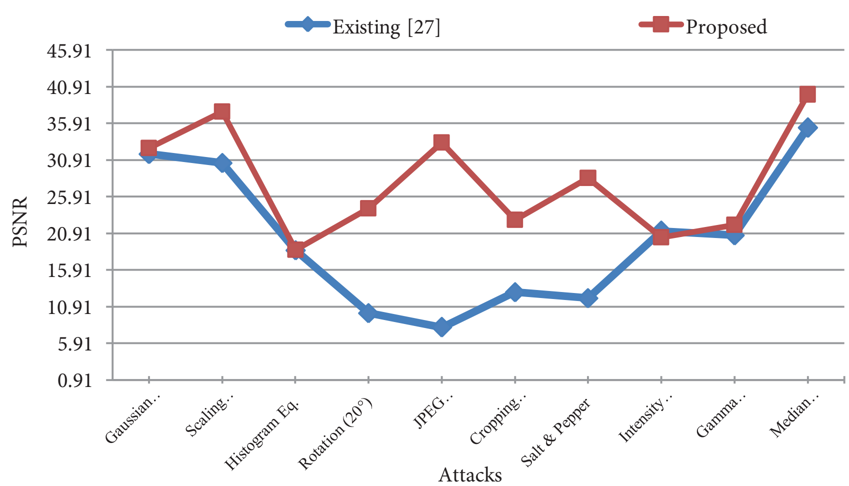

Figure 5. The PSNR comparison of the proposed and existing algorithm [27] for the noisy watermarked Pepper image.

The Pepper cover image offers better imperceptibility under all types of noise attacks except under the histogram equalization attack. In the case of histogram equalization, the imperceptibility measures of both schemes are quite close to each other, and this is depicted by graphical analysis in Figure 5. Moreover, under a JPEG compression attack the proposed scheme results in a PSNR value of more than 26 dB for both cover images, whereas the existing algorithm shows a PSNR value of around 8 dB. Figure 6 shows the visual quality of the Goldhill watermarked images under different noise attacks.

Comparative analysis of the NSR values of extracted watermark images under a variety of noise attacks are given in Table 2 for the Goldhill image, and graphical representation is given in Figure 7 for the Pepper image. From this analysis, it is clear that the proposed algorithm is better compared to the existing algorithm for both types of cover images against all attacks, with the exception of rotation and cropping attacks. Furthermore,

Figure 6. Goldhill watermarked images under noise attacks: a) Gaussian blur (3 × 3), b) scaling (1/2), c) histogram equalization, d) rotation (20°), e) JPEG (Q = 25), f) cropping (13%), g) salt and pepper (density = 0.01), h) intensity adjustment (1%), i) gamma correction (0.9), j) median filtering (3 × 3).

for Gaussian blur, scaling, and JPEG compression attacks, the proposed scheme presents an NSR value of 1, which shows a complete matching of the extracted watermark image with the embedded watermark image.

The visual qualities of the extracted watermark images are depicted in Figure 8. The respective NCC values of extracted watermark images under various attacks are given in Table 3. Both NCC and NSR parameters show similar results for the respective images. The proposed implementation of PSO does not significantly increase execution time as it takes a smaller number of iterations to reach the desired solution.

It is noteworthy that PSO is used as the optimization technique for selecting the scale factor in the proposed scheme. In contrast, in the approach found in [27], a suitable value of scale factor was manually selected.

The authors in [27] did not discuss execution time. The implementation of the scheme given in [27] on a machine with a 2.8 GHz core i5 processor with 4 GB RAM shows that the execution time for a single value of scale factor is 0.57 s. Since 10 different scale factors are used in [27], the total execution time needed to obtain a suitable scale factor ends up being 0.57 × 10 = 5.7 s.

Table 2. NSR comparison of the proposed and existing algorithm [27].

Attacks	NSR of the extracted watermark	
	Goldhill cover image	
	Reference [27]	Proposed
Gaussian blurring (3 × 3)	0.9946	1
Scaling (512–256)	0.9925	1
Histogram eq.	0.988	0.9956
Rotation (20°)	0.9883	–0.580
JPEG compr. (Q = 25)	0.9929	1
Cropping (13%)	0.9947	–0.277
Salt and pepper	0.9076	0.9895
Intensity adjustment	0.9936	0.9904
Gamma correction (0.9)	0.9990	1
Median filtering (3 × 3)	0.9986	1

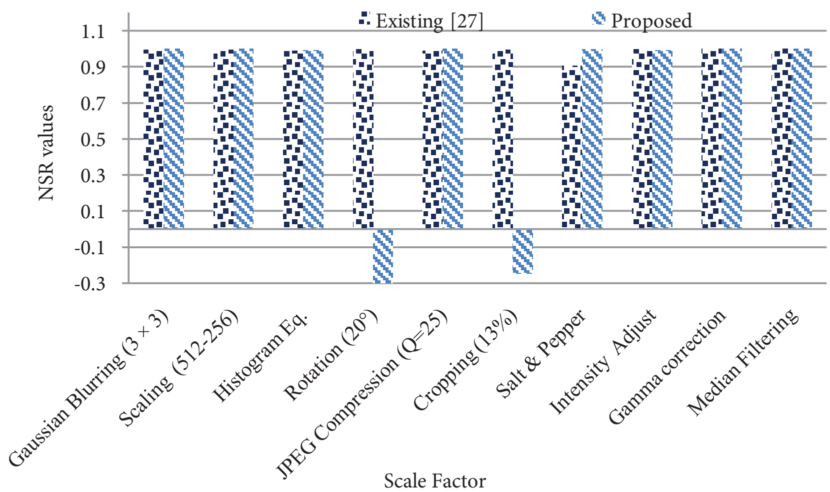

Figure 7. NSR value comparison of the proposed and existing algorithm for the extracted watermark image with Pepper as a cover image.

Table 3. NCC value of the extracted watermark from different noisy watermarked images with the proposed algorithm.

Attacks	NCC	
	Pepper image	Goldhill image
Gaussian blurring (3 × 3)	1	1
Scaling (512–256)	1	1
Histogram eq.	0.9933	0.9970
Rotation (20°)	0.0504	0.0489
JPEG compr. (Q = 25)	1	1
Cropping (13%)	0.2061	0.2014
Salt and pepper	0.9970	0.9927
Intensity adjustment	0.8644	0.9933
Gamma correction (0.9)	1	1
Median filtering (3 × 3)	1	0.9994

In the proposed scheme, five particles and eight iterations are used. It implies that our algorithm is required to be executed 40 times to get a suitable scale factor. The execution time for this process is 13.12 s.

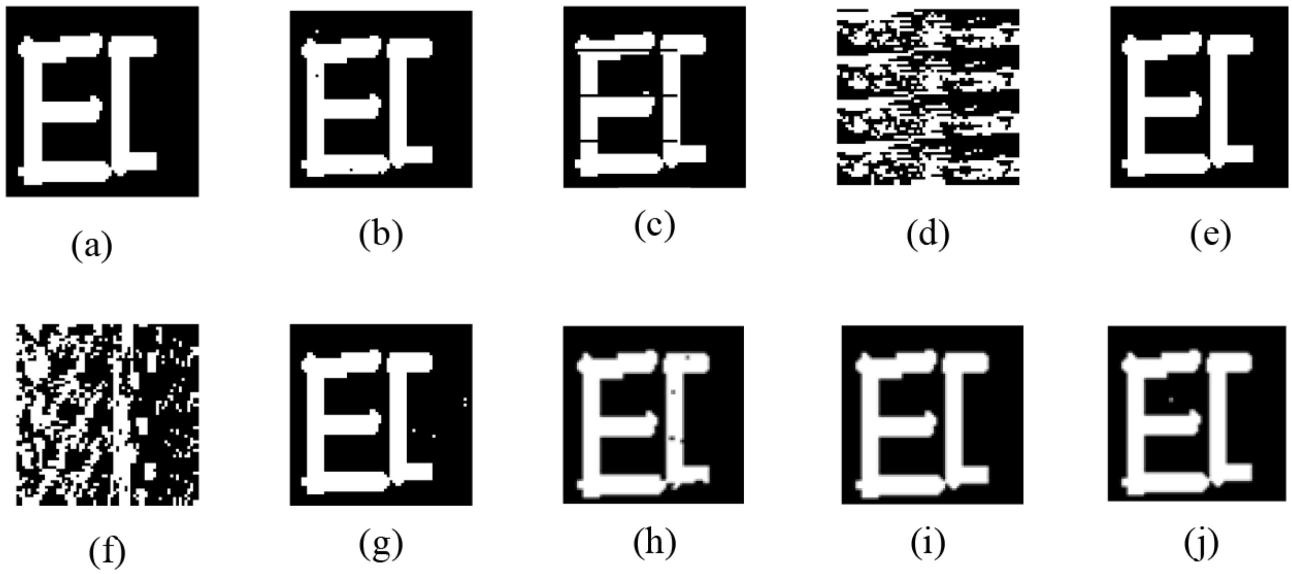

Figure 8. Extracted watermark from watermarked Goldhill image under various noise attacks: a) Gaussian blur (3 × 3), NSR = 1, b) scaling (1/2), NSR = 1, c) histogram equalization, NSR = 0.9956, d) rotation (20°), NSR= –0.580, e) JPEG (Q = 25), NSR = 1, f) cropping (13%), NSR= –0.277, g) Salt and Pepper (density = 0.01), NSR = 0.9895, h) intensity adjustment (1%), NSR = 0.9904, i) gamma correction (0.9), NSR = 1, j) median filtering (3 × 3), NSR = 0.9991.

The average value of execution time per execution cycle for the proposed scheme is relatively less at 0.328 s compared to 0.57 s, but the total execution time for the proposed scheme seems to be longer than that of the scheme in [27]. The effective execution time required by the scheme proposed in [27] is expected to be much larger due to the manual selection of the scale factor. However, the use of a constant scale factor in this scheme will reduce the effective execution time. This may be due to the blocking of subband LL of the cover image for watermark embedding.

The proposed algorithm is also tested for Cameraman, Lena, Baboon, and Boat host images to verify its generality toward different image data sets. The NSR and NCC values of the extracted watermarks using these images are given in Table 4. PSNR values of Cameraman, Lena, Baboon, and Boat noisy watermarked images are presented in Table 5. The results given in Tables 4 and 5 show that the proposed scheme also performs better using different sets of images such as Goldhill and Pepper. The results of comparison are mentioned in Table 6 using Lena as the cover image. This shows that the proposed algorithm performs better than the scheme proposed in [16] under all attacks except cropping and rotation.

6. Conclusion

In the proposed block-SVD-based approach, each watermark pixel is embedded into a singular value of each block of the LL wavelet subband of the cover image. The embedding locations are secret, which increases the security of the copyright content. Moreover, the proposed block-based approach removes the diagonal line problem presented in the extracted watermark in the existing algorithms [6,27]. In this scheme, automatic selection of a suitable scale factor for embedding a watermark into cover images is performed using PSO. This gives better robustness and imperceptibility to watermark and watermarked images, respectively. The PSNR values of noisy watermarked images and the NSR value of extracted watermark images for the proposed

Table 4. NCC and NSR values of the extracted watermark from different noisy watermarked images Cameraman, Lena, Baboon, and Boat with the proposed algorithm.

Attacks	Cameraman		Lena		Baboon		Boat	
	NCC	NSR	NCC	NSR	NCC	NSR	NCC	NSR
Gaussian blurring (3 × 3)	0.997	0.995	0.999	0.999	0.999	0.999	1	1
Scaling (512–256)	0.990	0.986	0.997	0.996	0.998	0.998	1	1
Histogram eq.	0.980	0.972	0.926	0.894	0.991	0.987	0.954	0.934
Rotation (20°)	0.148	–0.343	0.108	–0.545	0.043	–0.594	0.101	–0.516
JPEG compr. (Q = 25)	0.999	0.999	0.999	0.999	1	1	1	1
Cropping (13%)	0.177	–0.263	0.107	–0.551	0.200	–0.222	0.170	–0.276
Salt and pepper (0.01)	0.994	0.991	0.999	0.999	0.997	0.995	0.984	0.977
Intensity adjustment	0.881	0.831	0.838	0.771	0.955	0.935	1	1
Gamma correction (0.9)	1	1	1	1	0.963	0.947	1	1
Median filtering (3 × 3)	0.998	0.986	0.999	0.999	0.992	0.989	0.998	0.998

Table 5. PSNR values of noisy watermarked images Cameraman, Lena, Baboon, and Boat with the proposed algorithm.

Attacks	PSNR of watermarked images			
	Cameraman	Lena	Baboon	Boat
Gaussian blurring (3 × 3)	33.8568	35.7776	37.7999	37.1869
Scaling (512–256)	29.3836	31.7024	31.6779	33.3806
Histogram eq.	17.1329	16.3264	14.4691	14.9768
Rotation (20°)	10.2723	11.1514	11.9365	11.4893
JPEG compr. (Q = 25)	31.7835	31.2191	29.2820	31.5711
Cropping (13%)	14.6525	11.1830	16.2685	18.0349
Salt and pepper (0.01)	22.4702	23.9163	24.4397	24.5941
Intensity adjustment	19.3077	21.4496	20.0400	20.6114
Gamma correction (0.9)	24.2327	22.5266	27.8019	18.9821
Median filtering (3 × 3)	29.3369	29.4470	31.7627	37.4559

Table 6. NCC comparison of the proposed and existing algorithm [16].

Attacks	NCC of extracted watermark image	
	Proposed	Reference [16]
Rotation (10°)	0.1744	0.7554
Scaling (0.5)	1	0.8127
Gaussian noise (0.01)	0.9994	0.7716
Cropping (10%)	0.1774	0.8029
JPEG compr. (Q = 40)	1	0.9524
Low-pass filtering (3 × 3)	1	0.7849
Salt and pepper (0.01)	1	0.8916

scheme are better than the existing algorithm against most noise attacks. Under JPEG compression attack, the performance of the proposed algorithm, in terms of PSNR value, has improved compared to the existing algorithm by 25 dB and 18 dB for the Pepper and Goldhill cover images, respectively. Under this kind of attack, both the NSR and NCC values of the extracted watermark are 1, which shows perfect matching between the original and extracted watermark images. Therefore, the PSO-based optimization technique used for selecting a scale factor for watermark embedding in the proposed algorithm not only makes it adaptive but also improves the performance without a significant increase in computation complexity. Performance analysis shows that the proposed watermarking algorithm performs better for a wide variety of images. It may be interesting to analyze the proposed scheme with other existing optimization techniques (e.g., HPSO [28]) in order to obtain better performance. A blind, secure, and dual watermarking based on SVD in a DWT domain where the watermark image (for authentication) and electronic patient record data need to be embedded into the host medical image could be an interesting topic for future investigation.

References

[1] Liu R, Tan T. An SVD-based watermarking scheme for protecting rightful ownership. IEEE T Multimedia 2002; 4: 121-128.

[2] Bao P, Ma X. Image adaptive watermarking using wavelet domain singular value decomposition. IEEE T Circ Syst Vid 2005; 15: 96-102.

[3] Zhang X, Li K. Comments on: An SVD-based watermarking scheme for protecting rightful ownership. IEEE T Multimedia 2005; 7: 593-594.

[4] Rykaczewski R. Comments on: An SVD-based watermarking scheme for protecting rightful ownership. IEEE T Multimedia 2007; 9: 421-423.

[5] Jain C, Arora S, Panigrahi P. A reliable SVD based watermarking scheme. arXiv: 0808.0309.

[6] Lai C, Tsai C. Digital image watermarking using discrete wavelet transform and singular value decomposition. IEEE T Instrum Meas 2010; 59: 3060-3063.

[7] Mehta S, Nallusamy R, Maravar R, Prabhakaran B. A study of DWT and SVD based watermarking algorithm for patient privacy in medical images. In: IEEE 2013 International Conference on Healthcare Informatics; 9–11 September 2013; Philadelphia, PA, USA. New York, NY, USA: IEEE. pp. 287-296.

[8] Rezazadeh S, Rahmati M. A robust watermarking scheme based on wavelet transform and block SVD. In: IEEE 2007 International Symposium on Signal Processing and Its Applications; 12–15 February 2007; Sharjah, UAE. New York, NY, USA: IEEE. pp. 1-6.

[9] Mohammad A, Alhaj A, Shaltaf S. An improved SVD-based watermarking scheme for protecting rightful ownership. Signal Process 2008; 88: 2158-2180.

[10] Ghazy R, Hadhoud M, Dessouky M, El-Fishawy N, Abd El-Samie F. Performance evaluation of block based SVD image watermarking. Prog Electromagn Res 2008; 8: 147-159.

[11] Guo J, Prasetyo H. False-positive-free SVD-based image watermarking. J Vis Commun Image R 2014; 25: 1149-1163.

[12] Ghazy R, Abbas A, Al-Zubi N, Hassan E, El-Fishawy N, Hadhoud M, Dessouky M, El-Rabaie E, Alshebeili S, El-Samie F. Block-based SVD image watermarking in spatial and transform domains. J Electron 2014; 102: 1091-1113.

[13] Senol A, Dincer K, Sever H, Elbasi E. Block-DWT based vector image watermarking. In: IEEE Signal Processing and Communications Applications Conference; 16–19 May 2015; Malatya, Turkey. New York, NY, USA: IEEE. pp. 264-267.

[14] Dowling J, Planitz BM, Maeder AJ, Du J, Pham B, Boyd C, Chen S, Bradley AP, Crozier S. A comparison of DCT and DWT block based watermarking on medical image quality. In: Shi YQ, Kim HJ, Katzenbeisser S, editors. Digital Watermarking. Berlin, Germany: Springer, 2008. pp. 454-466.

[15] Wang Z, Sun X, Zang D. A novel watermarking scheme based on PSO algorithm. In: Li K, Fei M., Irwin GW, Ma S, editors. Bio-Inspired Computational Intelligence and Applications. Berlin, Germany: Springer, 2007. pp. 307-314.

[16] Tao H, Zain J, Abdalla A, Ahmed M. Hybrid particle swarm optimization for robust digital image watermarking. Int J Phys Sci 2011; 6: 7222-7232.

[17] Kumsawat P. A genetic algorithm optimization technique for multiwavelet-based digital audio watermarking. EURASIP J Adv Sig Pr 2010; 2010: 471842.

[18] Harrak H, Hien TD, Nagata Y, Nakao Z. DCT watermarking optimization by genetic programming. Adv Soft Comp 2006; 35: 347-351.

[19] Rao VSV, Shekhawat RS, Srivastava VK. A reliable digital image watermarking scheme based on SVD and particle swarm optimization. In: IEEE 2012 Students Conference on Engineering and Systems; 16–18 March 2012; Allahabad, India. New York, NY, USA: IEEE. pp. 1-6.

[20] Run R, Horng S, Lai J, Kow T, Chen R. An improved SVD-based watermarking technique for copyright protection. Expert Syst Appl 2012; 39: 673-689.

[21] Tao H, Zain JM, Abd Alla AN, Hongwu Q. Particle swarm optimization for digital image watermarking. In: Zhang Y, Cuzzocrea A, Ma J, Chung KI, Arslan T, Song X, editors. Database Theory and Application, Bio-Science and Bio-Technology. Berlin, Germany: Springer, 2010. pp. 1-8.

[22] Tsai HH, Jhuang YJ, Lai YS. An SVD-based image watermarking in wavelet domain using SVR and PSO. Appl Soft Comput 2012; 12: 2442-2453.

[23] Kuppusamy K, Thamodaran K. Optimized image watermarking scheme based on PSO. In: International Conference on Modeling Optimization and Computing; 10–11 April 2012; Kumarakoil, India. pp. 493-503.

[24] Aslantas V, Dogan AL, Ozturk S. DWT-SVD based image watermarking using particle swarm optimizer. In: IEEE International Conference on Multimedia and Expo; 23 June–26 April 2008; Hannover, Germany. New York, NY, USA: IEEE. pp. 241-244.

[25] Ganic E, Eskicioglu A. Robust DWT-SVD based watermarking: embedding data in all frequencies. In: ACM 2004 workshop on Multimedia and Security; 20–21 September 2004; Magdeburg, Germany. pp. 166-174.

[26] Kennedy J, Eberhart R. Particle swarm optimization. In: IEEE 1995 International Conference on Neural Networks; November–December 1995; Perth, Australia. New York, NY, USA: IEEE. pp. 1942-1948.

[27] Jane O, Elbasi E, Ilk H. Hybrid non-blind watermarking based on DWT and SVD. J Appl Res Technol 201; 12: 750-761.

[28] Surekha P, Sumathi S. Performance comparison of optimization techniques on robust digital-image watermarking against attacks. Appl Artif Intell 2012; 26: 615-644.